Evaluation of a Tissue-Engineered Membrane-Cell Construct for Guided Bone Regeneration

Jan-Thorsten Schantz, MD[1]/Dietmar Werner Hutmacher, M Eng, PhD, MBA[2]/Kee Woei Ng, M Eng[3]/Hwei Ling Khor, M Eng[4]/Thiam Chye Lim, MD[5]/Swee Hin Teoh, PhD[6]

Purpose: *Currently, a number of bioresorbable and biodegradable membranes used for guided bone regeneration lead to incomplete tissue regeneration. Poor mechanical properties, short degradation time, and the lack of integrated biologic components result in the inability to create and maintain an appropriate environment and to actively support tissue remodeling. In the present study, the osteogenic potential of human calvarial periosteal cells in combination with ultrathin polycaprolactone (pc2) membranes of a slow biodegradation rate was investigated.* ***Materials and Methods:*** *In vitro and in vivo analyses of the tissue-engineered constructs were conducted using imaging techniques, immunohistochemistry, and histology. Two types of membranes were investigated. Group 1 consisted of a plain membrane, and in group 2 membranes were treated with sodium hydroxide.* ***Results:*** *In vitro results showed that osteoblast-like cells attached and proliferated on the membranes with the formation of extracellular matrix. Sodium hydroxide–treated membranes showed enhanced cell attachment and proliferation kinetics, resulting in a dense cellular layer after 2 weeks in culture. In vivo mineralized tissue formation in association with vascularization was observed. Extracellular matrix calcification with nodule formation was detected via histology as well as scanning electron microscopy.* ***Discussion:*** *PCL membranes support the attachment, growth, and osteogenic differentiation of human primary osteoblast-like cells. Sodium hydroxide–treated membranes demonstrated increased cell attachment resulting from increased hydrophilicity.* ***Conclusion:*** *These findings have potential application in the development of a new generation of osteoconductive membranes.* (Int J Oral Maxillofac Implants 2002;17:161–174)

Key words: *guided bone regeneration, periosteal cells, polycaprolactone membrane, tissue engineering*

[1]Research Fellow, Laboratory for Biomedical Engineering and Division of Plastic Surgery, Department of Surgery, National University of Singapore, Singapore.
[2]Assistant Professor, Department of Bioengineering and Department of Orthopaedic Surgery, National University of Singapore, Singapore.
[3]Research Engineer, Division of Plastic Surgery, Department of Surgery, National University of Singapore, Singapore.
[4]Research Engineer, Laboratory for Biomedical Engineering and Department of Mechanical Engineering, National University of Singapore, Singapore.
[5]Associate Professor and Head, Division of Plastic Surgery, Department of Surgery, National University Hospital, Singapore.
[6]Associate Professor and Director, Laboratory for Biomedical Engineering and Department of Bioengineering, National University of Singapore, Singapore.

Reprint requests: Dr Jan-Thorsten Schantz, Laboratory for Biomedical Engineering and Division of Plastic Surgery, Department of Surgery, National University of Singapore, 10 Kent Ridge Crescent, Mechanical Engineering, 119260 Singapore. Fax: +65-777-3537. E-mail: mpejts@nus.edu.sg

Presented at the International Workshop on Bone Substitutes, Davos, Switzerland, October 8–10, 2000, and the 10th International Conference on Biomedical Engineering, Singapore, December 5–9, 2000.

Over the last decade, extensive experience has been gained by implementing the guided bone regeneration (GBR) technique in clinical treatment regimes. The objective of GBR is to promote bone formation in osseous deformities, either before or in conjunction with endosseous implant placement. Osseous defects consist mainly of extraction sites, dehiscences, and/or fenestrations, as well as localized ridge defects. Furthermore, bone defect geometry may either provide natural spacemaking or be nonspacemaking. At present, the GBR technique is supported by a significant number of experimental and clinical studies, randomized and nonrandomized.[1–3] The clinical goal of GBR is to create a suitable environment in which the natural biologic potential for functional regeneration can be maximized. [4–7]

It has become clear that tissue separation is only one of many interacting factors that influence the predictability and success of GBR treatment procedures. Important factors involved in the creation of a suitable environment for GBR procedures include: biomechanical stability of the resolving wound complex, prevention of acute inflammation resulting

from bacterial infection, isolation of the regenerative space from undesirable competing tissue types, and creation and maintenance of a blood clot–filled space.[8] While certainly not the only critical component to successful GBR treatment, the material properties and membrane design employed in the therapy can significantly influence all of the above-mentioned factors.[9] However, membranes made purely of synthetic or natural polymers without biologic components permit only passive tissue regeneration.[10]

Bone generation by autogenous cell culturing and transplantation is one of the most promising treatment concepts being developed in the area of reconstructive surgery.[11] Osteoblast-like cells obtained from an individual patient can be grown in culture and seeded onto a scaffold that will slowly degrade and resorb as the bone structures are formed and assimilate in vivo with the host tissue. The scaffold provides the necessary support for cells to maintain their differentiated state and defines the overall shape of the tissue-engineered transplant.[12]

Tissue-engineering concepts have not yet been applied for the development of membrane-cell constructs whose physical and biologic properties permit not only passive host tissue integration, but also have desirable cell types and tissue components that actively produce bone. In this study, the concept of combining the cellular component with a bioresorbable membrane was evaluated both in vitro and in vivo.

MATERIALS AND METHODS

Specimens

Polycaprolactone (PCL) films were fabricated as described by Ng and associates.[13] Briefly, PCL thin films were prepared using a standard solution-casting method. PCL pellets (Mn 80 000, Sigma-Aldrich, St Louis, MO) were dissolved in methylene chloride (6% by weight) and cast onto glass sheets. The solvent was removed by slow evaporation. The films were further dried in vacuum at room temperature for 2 days. Films of diameter 210 mm with a thickness of 100 to 110 μm were obtained. A laboratory press (Dr Collin GmbH, Ebersberg, Germany) with 4 columns and a plated area of 36 square inches was used. The heat press process was necessary to improve film uniformity and to reduce defects that would negatively influence the biaxial drawing process. All pressed films were placed in ice water immediately after removal from the hot press. The pressed films were then cut to 7 × 7 cm for biaxial drawing. The films were biaxially drawn using a biaxial drawing apparatus designed and built in-house.[13]

All samples were processed using a drawing speed of 200 mm/min and a draw ratio of 3 × 3. Thin transparent film specimens were obtained after drawing. For this study, the films were 10 ± 2 μm thick. The surface morphology was studied via scanning electron microscopy (SEM) and atomic force microscopy (AFM) as described by Ng and associates.[13] Representative scans from 3 different films of each group were collected. Circular films of 16 mm diameter were stamped out from the rectangular PCL sheet using a hollow stainless steel punch (Elora, Remscheid, Germany). One group of PCL films was treated with sodium hydroxide (NaOH) solution for 3 hours to render the PCL films more hydrophilic. The specimens were grouped as follows: *(1)* PCL films, untreated, *(2)* PCL films, NaOH-treated. For NaOH treatment, the PCL films were soaked in 30 mL of 5 mol/L NaOH (JT Baker, Phillipsburg, NJ) for 3 hours. The films were washed 3 times in phosphate-buffered saline (PBS) and sterilized. For sterilization, all specimens were soaked in ethanol (Merck, Darmstadt, Germany) for 24 hours. They were then washed twice with PBS, placed into 6 well plates, and dried in an incubator at 37°C and 5% carbon dioxide for 1 hour.

In Vitro Study

All media, supplements, and chemicals were purchased from Gibco (Life Technologies, Grand Island, NY) and Sigma-Aldrich unless otherwise stated in the text. Biopsies from human calvarial periosteum were harvested under sterile conditions and placed in Ringer's solution. Samples were cut into 1.0 × 1.0-cm pieces and extreme care was taken when the inner cambial layer was separated from the outer fibrous sheet. An explant culture system was established to isolate the osteoblast precursor cells from the cambial layer.[14] Cells were amplified in monolayer cultures and passaged twice using Gibco M199 culture media with 10% FBS and 1% penicillin-streptomycin. Prior to cell-seeding, 80% confluent cultures were enzymatically lifted from the T75 flask with 0.05% trypsin-EDTA (Hyclone, Logan, UT) and counted with a hemocytometer. Cell viability was assessed with Trypan blue staining.

On average, 50,000 osteoblast-like cells were seeded per film in 4 different areas to achieve a homogenous cell distribution. The seeded films were then left for 30 minutes in the incubator at 37°C and 5% carbon dioxide for cell attachment to occur. A glass ring 14 mm in diameter was placed on each specimen to weigh down the films, so as to prevent them from floating on the media. The samples were then carefully topped with 2 mL of culture media supplemented with 50 μg/mL ascorbic acid and 10 mmol/L beta-glycerolphosphate to

induce the osteoblastic phenotype. Constructs were kept in culture for 2 weeks prior to implantation.

Phase Contrast Light and Scanning Electron Microscopy. Establishment of the osteoblast-like morphology of intercellular connections and qualitative cell proliferation over time were examined daily by phase-contrast light microscopy for 2 weeks. Adhesion of the cells to the PCL foil and their distribution were studied via SEM. Specimens were fixed in 2.5% gluteraldehyde (Merck) for at least 4 hours at 4°C. They were then dehydrated in a graded ethanol series of 30%, 50%, 90%, and 100% for 5 minutes at each grade; dried; and examined with a Jeol JSM-5800LV SEM (Tokyo, Japan) at 15 kV.

Confocal Laser and Fluorescence Microscopy. The cell-membrane constructs were prepared for confocal laser microscopy (CLM) by staining viable cells green with the fluorescent dye fluorescein diacetate (FDA) (Molecular Probes, Eugene, OR). The 3D cultures were incubated at 37°C with 2 µg/mL FDA in PBS for 15 minutes. After rinsing twice in PBS, each sample was placed in 1 mg/mL propidium iodide solution (Molecular Probes) for 2 minutes at room temperature to stain dead cells red. The samples were then rinsed twice in PBS and viewed under a CLM (Olympus IX70-HLSH100 Fluoview, Tokyo, Japan). Depth projection images were constructed from up to 25 horizontal image sections through the cultures.

For fluorescence microcopy, membrane-cell constructs were first fixed in 3.7% formaldehyde at room temperature for 30 minutes. After rinsing twice with PBS for 5 minutes each time, 200 µg/mL RNAse A was added and left for 30 minutes at room temperature. Phalloidin (A12379 Alexa Fluo 488 phalloidin, Molecular Probes) was then added in at a 1:200 dilution for 45 minutes at room temperature and in darkness. Samples were subsequently counterstained with 5 µg/mL propidium iodide solution, dried, and mounted for viewing under fluorescence microscopy.

Osteocalcin Assay. The supernatant from stimulated membrane-cell constructs was collected after 1 week and after 2 weeks and immediately frozen at –80°C. Prior to analysis, 10 µL of each sample was brought to room temperature and dissolved in 1 mL assay buffer. The quantity of human osteocalcin was determined using an enzyme-linked immunosorbent assay (ELISA) (DSL-10-7600 Active Human Osteocalcin ELISA Kit, Diagnositc Systems Laboratories, Webster, TX). All tests were performed in quadruplicate.

In Vivo Study

Surgical Procedure. The animals were housed in the animal holding facility, Department of Experimental Surgery, National University Hospital, for the entire duration of the experiment. Housing and feeding were done according to standard animal care protocols. The studies had been approved by the Animal Welfare Committee of the National University of Singapore and had been licensed by the National Institute of Health's Guide for Care and Use of Laboratory Animals. Implantation of experimental and control specimens was performed under sterile conditions in a laminar flow hood.

Six male athymic Balb C nude mice, 6 to 8 weeks old, weighing between 20 to 22 g each, were used for the in vivo study, in accordance with the animal care guidelines. The mice were anesthetized with 0.15 mL of an anesthetizing cocktail (Dormicum and Hypnorm 1:1) injected intraperitoneally before the operation. The backs of the mice were prepared with iodine and 70% alcohol, and the animals were placed in a prone position on the table. The tissue-engineered membrane-cell constructs were inserted into subcutaneous pockets, with NaOH-treated samples placed on the left and untreated samples on the right paravertebral side. The cell-seeded side of the transplant was placed facing toward the skin of the animals. The wound was then closed with interrupted 5/0 Prolene sutures (Ethicon, Somerville, NY) and wound sites were sprinkled with an antibiotic powder. The mice were euthanized after 4 months using carbon dioxide asphyxiation and the implants were harvested with a small rim of surrounding soft tissue.

Histology and Immunohistochemistry. The main part of the explanted specimens was fixed in Schaffers solution and embedded in polymethyl methacrylate (PMMA) (Technovit 9100 Heraeus/Kulzer, Wehrheim, Germany). Five-micron-thick sections were cut using a mycrotome (Leica RM 2165, Bensheim, Germany) and mounted on poly L-lysine (Sigma)–coated slides. Sections were deplastified by submerging the slides for 20 minutes in 98% 2-methoxyethyl-acetate (Merck) followed by a decreasing ethanol series. Slides were stained with von Kossa silver nitrate and toluidine blue.

Immunohistochemistry with antibodies raised against the human HLA 1 epitope, osteocalcin, and alkaline phosphatase was carried out on undecalcified sections. Slides were incubated in humidified chambers for 1 hour at 37°C with the primary antibodies. For identification and separation of mouse and human tissue, slides were incubated with monoclonal antibodies raised against the human HLA 1 ABC Epitope (Clone W 5/32 Mouse Anti-Human, Dako, Glostrup, Denmark). Nonspecific sites of the antibody were shut off with a peroxidase block. Primary antibodies were detected with a 3,3-diaminobenzidine substrate and a chromogen peroxidase system

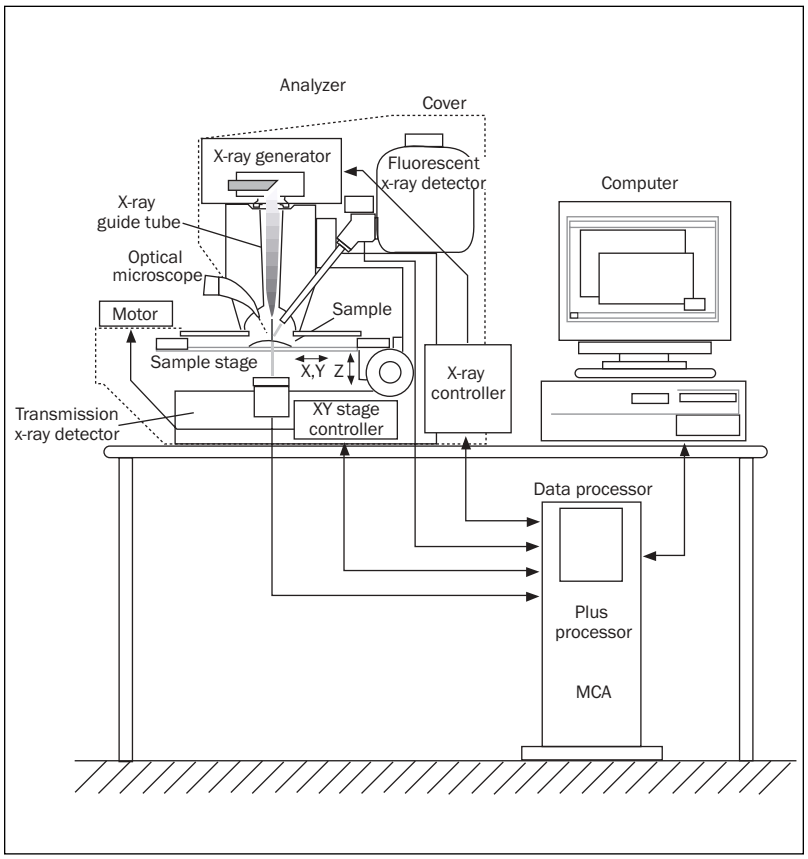

Fig 1 The XSAM. The x-rays generated in the x-ray tube are converged into a very thin x-ray beam with the x-ray guide tube (XGT). The beam is irradiated to the sample while its surface is being scanned. The transmitted image of the sample and the distribution images of its elements are then obtained. The measurement data and the position information obtained when the sample was scanned are used to form an image with the data processor and then display it.

(Dako EnVision+ System Peroxidase DAB, Hamburg, Germany). Counterstaining was performed with Gills hematoxylin (Sigma). Positive and negative controls were carried out on murine osteoblasts (negative) and human osteoblasts (positive) fixed cultures.

Osteocalcin immunostaining was carried out to further evaluate the tissue mineralization and calcification processes. Monoclonal mouse anti-human/bovine osteocalcin antibody (Biodesign, Saco, ME) was used in a dilution of 1:100. Slides were then incubated with a peroxidase-labeled polymer in which a secondary antibody is linked (Dako En Vision Peroxidase DAB). Then counterstaining with Gills hematoxylin was performed as described above. As a control, the peroxidase-labeled polymer was used alone for staining the microtomed sections.

X-ray Scanning Analytic Microscope. The residual part of the explanted specimens was used for x-ray scanning analytic (XSAM) microscopy (XGT-2000W, Horiba, Kyoto, Japan) (Fig 1). Elemental mapping images can be obtained for 11 Na to 92 U by energy dispersion of a fluorescent x-ray spectrum with a 2-dimensional resolution up to 10 μm.[15] In addition, x-ray transmission images were obtained. The transmission image and elemental mapping were obtained by mechanically scanning the sample under atmospheric pressure. Beams were generated from an unfiltered Rh-target x-ray guide tube. The aperture was set to a tube voltage of 30 kV with a current of 1 mA. The pulse processing time was set to a maximum of P4 with a live time per frame of 900 seconds. The analyzed spot size was between 2 and 3.5 mm. The mapping image with a resolution of 512 × 512 pixels was obtained for each specimen.

Gel Permeation Chromatography. The polymer molecular weight distribution was determined by gel permeation chromatography (GPC) equipped with a differential refractor (Waters, Model 410, Milford, MA) and an absorbance detector refractor (Waters, Model 2690). The samples were dissolved in tetrahydrofuran (THF) and eluted in a series of configurations through a Styragel columns refractor (Waters) at a flow rate of 1 mL/min. Polystyrene standards (Polyscience, Warrington, MA) were used to obtain a calibration curve.

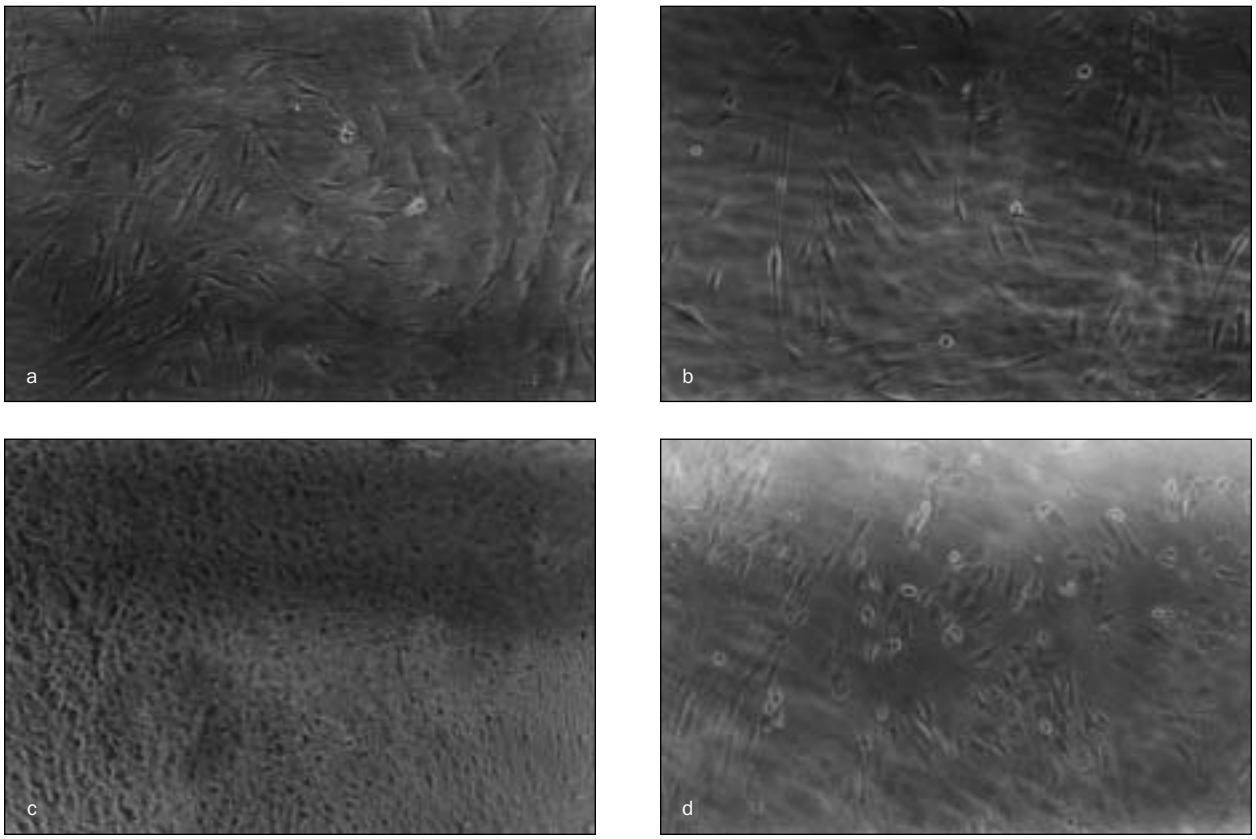

Figs 2a to 2d Live, nonstained periosteal cells of passage 3 proliferating on NaOH-treated (Figs 2a and 2c) and nontreated (Figs 2b and 2d) PCL films are shown as photographed with phase-contrast optics after 1 week (2a and 2b, original magnification ×100) and after 2 weeks (2c and 2d, original magnification ×40) under static culture conditions. The cell lawn became increasingly dense reaching confluency at day 14 for NaOH-treated specimens (Figs 2a and 2c). A lower cellular density and focal areas with apoptotic cells were detected on untreated membranes (Figs 2b and 2d). Periosteal cells presented extensive cell-to-cell contacts on NaOH-treated membranes in combination with a polygonal morphology (Fig 2a), whereas cells on untreated films appeared in a scholar-fish shape (Fig 2d).

RESULTS

In Vitro Study

Cell attachment was observed via phase-contrast light microscopy to start 3 hours after seeding the cell suspension on the PCL films. The initial cell attachment was higher on the treated samples when compared to the untreated samples, and cells spread out to a greater extent on the surface of the NaOH-treated PCL films. The osteoblast colonies started to migrate in radial patterns and proliferate into larger circular cultures over time. The complete film surface was covered on the NaOH-treated specimen by a homogeneous confluent cell lawn after 2 weeks in a static culture environment (Fig 2a). The untreated films still showed cell-free areas after 2 weeks (Fig 2b). On untreated films, osteoblasts showed a spindle-shaped, fibroblast-like morphology, changing their alignment to a scholar-fish formation at the onset of confluency (Fig 2d). The cells on the NaOH-treated films were initially more polygon-shaped (Figs 2a and 2c) compared to the elongated configuration on the untreated samples (Figs 2b and 2d). It was observed via daily phase-contrast microscopy that cell proliferation was qualitatively higher on the treated films.

Under the CLM, it was observed that a high percentage of cells were viable after 1 week (Figs 3a to 3d), with an increasing number of apoptotic cells after 2 weeks of culturing for both groups (Figs 3e and 3f). There were more dead cells found on the untreated films than on the NaOH-treated specimens. In apoptotic cells, nuclei were stained bright red and the classic progression of chromatin condensation and nuclear fragmentation was visible. Apoptosis markedly increased up to week 2, predominantly on the untreated specimens. The apoptosis might have been triggered by cell contact growth inhibition, because a multiple-layer morphology was observed, especially after 2 weeks in culture (Figs 3e and 3f).

Phallodin staining revealed that cells exhibited a dense f-action filament cytoskeleton after 1 week in culture (Figs 4a and 4b). The formation of focal

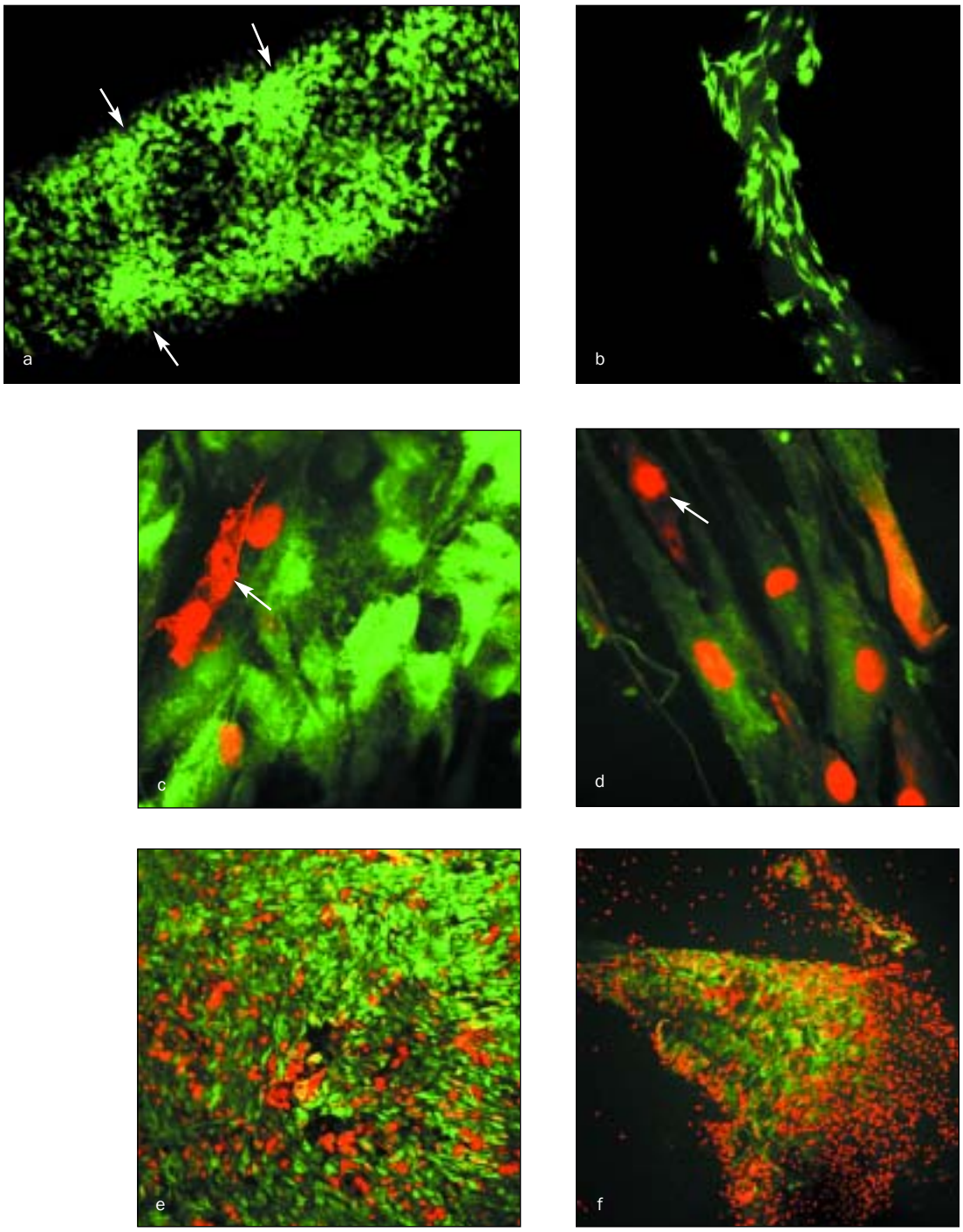

Figs 3a to 3f A series of confocal laser and fluorescence microscopy images of periosteal cells on untreated and treated PCL films after 1 and 2 weeks in culture. Living cells are stained bright green with FDA, while nuclei of apoptotic cells and cytoplasm of dead cells are counter-stained red with propidium iodide (Figs 3c and 3d). Periosteal cells formed a high number of dense colonies after 7 days in culture on the NaOH-treated PCL films (Fig 3a, *arrows;* original magnification ×40) whereas nontreated specimens (Fig 3b, original magnification ×40) showed a random cell distribution. This was confirmed by viewing representative samples of each group at higher magnifications (Figs 3c and 3d, original magnification ×200). At day 14 (Figs 3e and 3f, original magnification ×100) more dead cells are seen on PCL films of both groups. However, qualitative comparison allows the conclusion that the amount of deceased cells is higher on the untreated specimens when compared to the NaOH-treated PCL films.

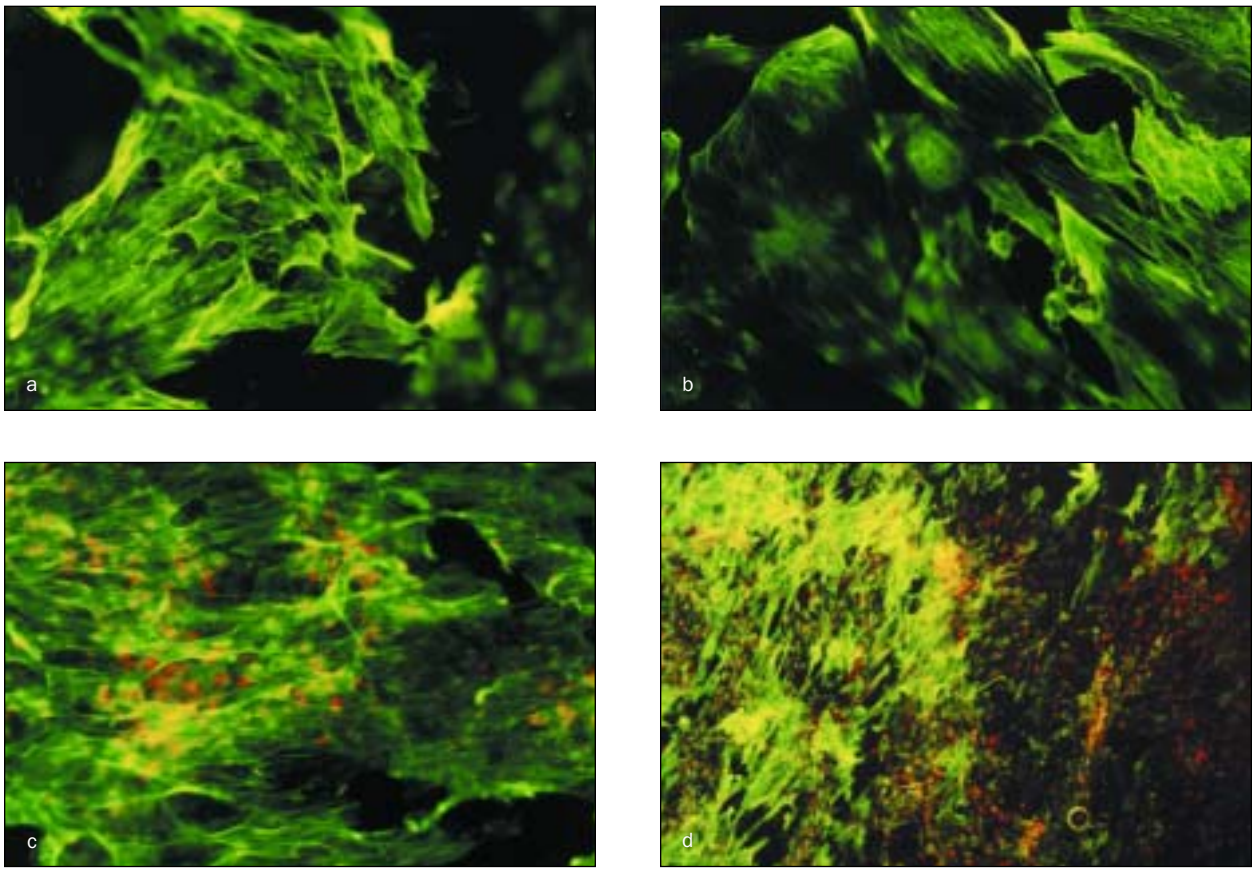

Figs 4a to 4d Cell morphology and attachment were studied by labeling the actin cytoskeleton with phalloidin and counterstaining the cell nuclei with propidium iodide. On fluorescence microscopy, images of 1-week specimens (Figs 4a and 4b, original magnification ×100), show a prominent f-actin fiber-network, with a higher amount of f-actin filaments in the NaOH-treated group, compared to the nontreated specimens. In accordance with the phase-contrast and SEM images, a difference in cell density for the treated and nontreated group was noticeable after 2 weeks (Fig 4c and 4d, original magnification ×40).

adhesions (stress fibers) increased during the 2 weeks in culture, with the NaOH-treated samples presenting a significantly denser network (Figs 4c and 4d). Again the osteoblasts formed multiple layers in the interior of the circular colonies. Osteoblast-specific osteocalcin production in the supernatant showed no obvious differences between the groups. The basal osteocalcin synthesis on the periosteal cell–seeded constructs ranged from 1.5 to 3.8 ng/mL. There was no significant difference in secretion either after week 1 or week 2 in culture between the groups. Cells on treated films produced the highest amount of osteocalcin after 1 week, with 3.7 ± 0.2 ng/mL. Levels on untreated films were 2.4 ± 0.2 ng/mL after week 1 and week 2, respectively.

SEM demonstrated osteoblast-like cells within a dense extracellular matrix in vitro. It was observed that the cells on the untreated films showed a proliferation pattern in which the osteoblast-like cells were aligned parallel to each other (Fig 5b). In contrast, cells on the NaOH-treated surface grew in a more random orientation, protruding toward the circular shape of the PCL foil (Fig 5a). In week 1, osteoblast-like cells in both groups showed features suggestive of well-attached cells, such as numerous dorsal membrane ruffles and microvilli (Figs 5a and 5b). However, after 2 weeks in culture, cells subsequently spread over the whole NaOH-treated PCL foil, forming confluent cellular multilayers in combination with a strong extracellular matrix (ECM) production (Figs 5c and 5d). Yet on untreated PCL films, cell-free areas and apoptotic and as well as detached ECM bundles were present after 2 weeks (Fig 5d).

In Vivo Study

Macroscopic Appearance. All the mice tolerated the surgical procedures and implantation well, showing only the expected mild inflammation from the wound healing response. Impaired wound healing or a clinically detectable foreign body reaction was not

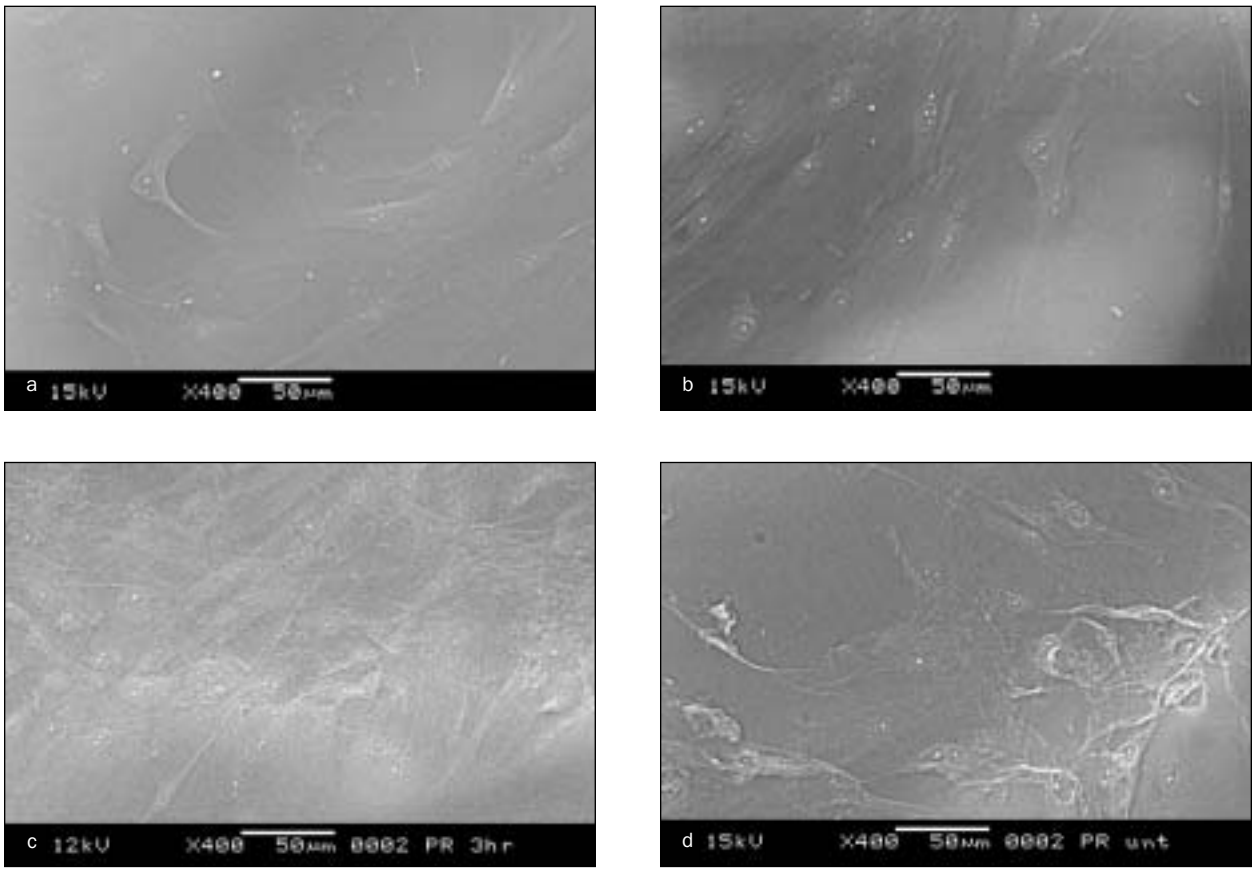

Figs 5a to 5d Scanning electron micrographs (original magnification ×400) showing cells growing on NaOH-treated (Figs 5a and 5c) and on untreated films (Figs 5b and 5d) after 1 and 2 weeks, respectively. Cells attached to the membranes via fillipodia and fiber-like processes. Features suggestive of cell activation with respect to cell-substrate interaction, including dorsal ruffles and microvilli-type elements, are partially present on the cells. The cells shown present this characteristic growth pattern with circular formation on NaOH-treated specimens (Fig 5a), whereas cells on untreated samples proliferated in a parallel alignment (Fig 5b). After 2 weeks, a higher amount of extracellular matrix (ECM) deposition could be observed throughout the entire treated film surface. In contrast, the nontreated specimens showed only random ECM formation.

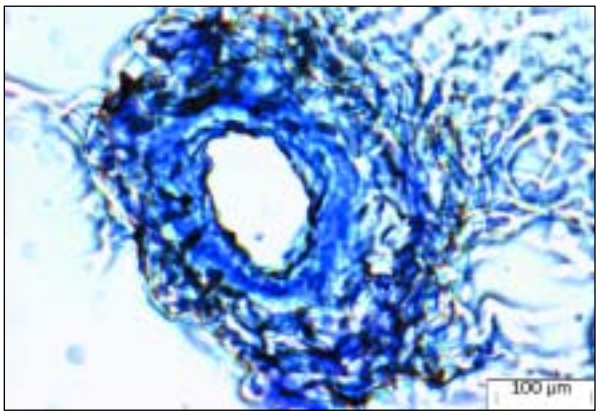

Fig 6 Gross morphologic observation (data not shown) of the vascularization of the fresh explanted specimens of both groups was confirmed via histology. Microvascular structures could be detected in the toluidine blue–stained cross section (original magnification ×200).

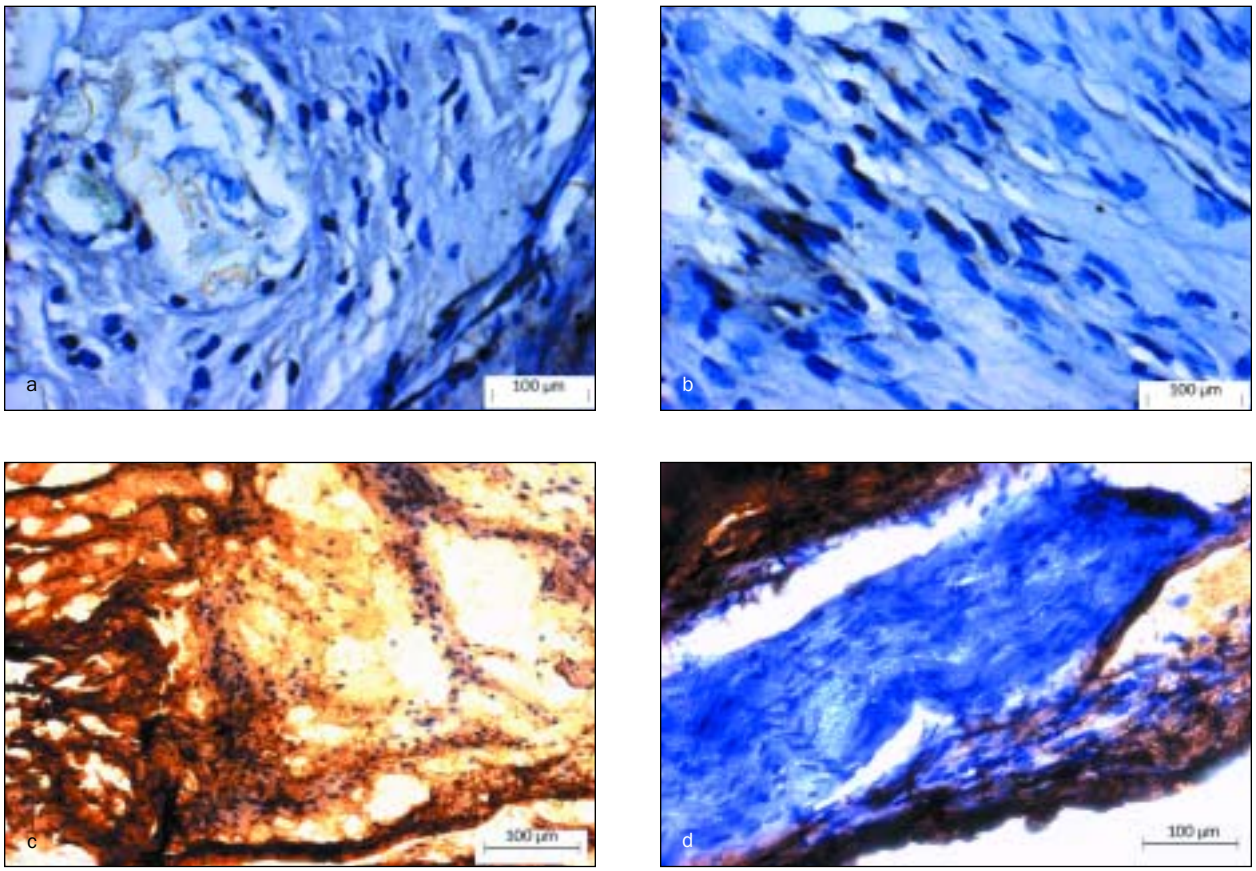

Figs 7a to 7d Immunohistochemical analysis was performed on deplastified sections of explanted specimens, and representative micrographs (original magnification ×100) were captured. The NaOH-treated PCL films showed a polygonal, loosely and randomly organized tissue structure in the osteocalcin (Fig 7a) and HLA Class I antigen (Fig 7c) staining. In contrast, explants of the untreated group revealed a scholar-fish–like and parallel cell formation of the cells within the collagen bundles for both types of staining (Figs 7b and 7d). Focal clusters of osteocalcin-positive cells were surrounded by murine fibrous tissue (Fig 7a, magnification ×100). In the internodular regions, loose cell formations were identified as HLA negative (blue stained cytoplasm).

seen at any time. Seventeen weeks after implantation, the tissue-engineered grafts could be clearly seen on the back of the mice. Two areas of increased firmness could be palpated on the skin of the mice. Tissue-engineered constructs of both groups could be excised at the time of harvesting. Upon gross examination, the implants appeared well integrated into the surrounding host tissue. The original dimension of the PCL films could still be detected within all of the explanted specimen. Macroscopically, fibrous tissue encapsulation or fibrotic reaction was not detected in any of the specimens.

Histology and Immunohistochemistry. Microscopically, no prominent foreign-body reaction was apparent in the surrounding mouse tissue. A narrow zone of fibrous connective tissue, which was HLA-negative in the immunostaining, indicating murine origin, surrounded the films. The membranes were lined with a dense cellular layer including multiple vascular structures (Fig 6). The HLA staining revealed that islands of connective tissue of mouse origin were present, partially disrupting the primary osteoblast cell lawn. Sparse areas of mineralized nodule formation were found, predominantly on the treated samples. The assessment of osteocalcin showed that HLA-positive cells expressed basal activity of the osteoblast-specific marker, which characterized them as osteoblast-like cells. The structural morphology of the explanted periosteal-membrane constructs showed 2 distinct tissue formation patterns. On NaOH-treated samples, osteoblast-like cells surrounded a core of collagen-rich matrix in a nodule-like fashion (Figs 7a and 7c). The matrix was mineralized as shown in Figs 8a and 8b. Tissues on untreated specimens presented a stretched muscular tissue–like appearance (Figs 7b and 7d) similar to the observed

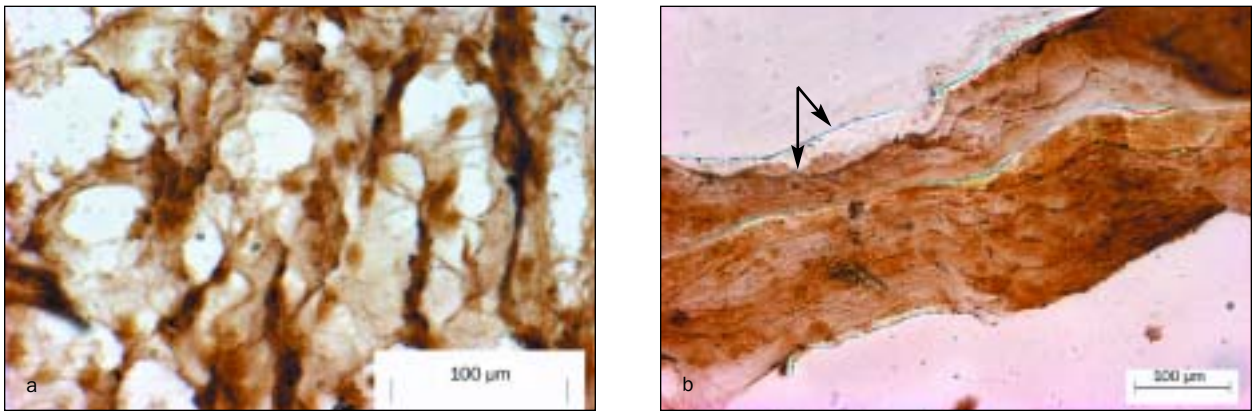

Figs 8a and 8b Photomicrographs (original magnification ×100) of representative histologic sections after von Kossa staining illustrate the different forms of tissue formation for both groups. Homogeneous formation of mature bone tissue was not seen for both groups. Onset of ECM mineralization was indicated for both groups by randomly distributed dark brown regions. However, NaOH-treated specimens (Fig 8a) revealed bigger tissue areas, which reacted with silver nitrate when compared to the nontreated PCL film group. In general, the sectioning of the tissue-engineered film/cell constructs was difficult due to the physiochemical properties of PCL. However, some sections allowed the detection of the tissue–PCL film interface (Fig 8b, *arrows*).

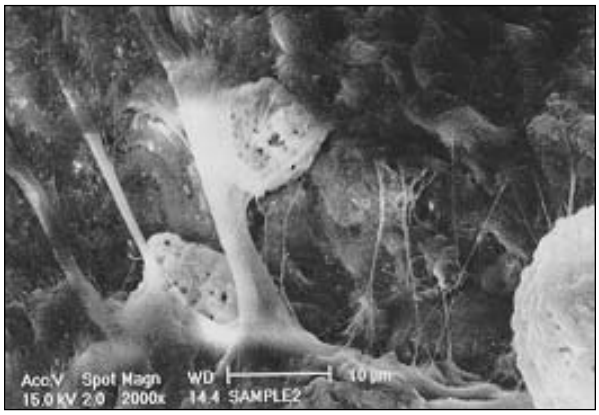

Fig 9 After 17 weeks of implantation, SEM (original magnification ×2,000) of NaOH-treated PCL film/cell constructs showed multiple mineralized globuli *(arrows)*, consisting of rounded cells embedded in a spider-like network of calcified extracellular matrix.

cell growth behavior in vitro (see Fig 2d). The membrane was penetrated by a vascular structure shown on the postoperative SEM and on the toluidine blue–stained section.

SEM and XSAM. In vivo morphologic characteristics indicated significant differences between the 2 groups, with prominent 3-dimensional cellular structures appearing as mineralized extracellular matrix (nodules) on the NaOH-treated films. The nodules consisted of rounded cells located in a spider-like network of extracellular matrix (Fig 9). Globuli were preferentially located around the central surface ridge of the specimen, where the vascular structure penetrated the membrane. The untreated films presented a dense, relatively uniform flat lawn of tissue. Uneven, more 3-dimensional tissue structures with globuli (mineralized nodules) were not observed.

Element distribution in the axial planes of the scanned specimens showed irregular patterns of calcium and phosphate deposition. Calcium- and phosphate-enriched spots were localized, particularly in the treated specimens (Fig 10a), whereas the untreated samples showed no focal enrichment (Fig 10b). The relative elemental concentration in the single spot analysis revealed that Ca reached a maximum x-ray intensity of 23.7 in the treated specimen compared to 1.8 in the untreated group. Phosphorous distribution partially overlapped the Ca mapping images. X-ray intensities ranged from 37.1 in the focal enriched spot on the treated sample to 4.3 in the untreated film.

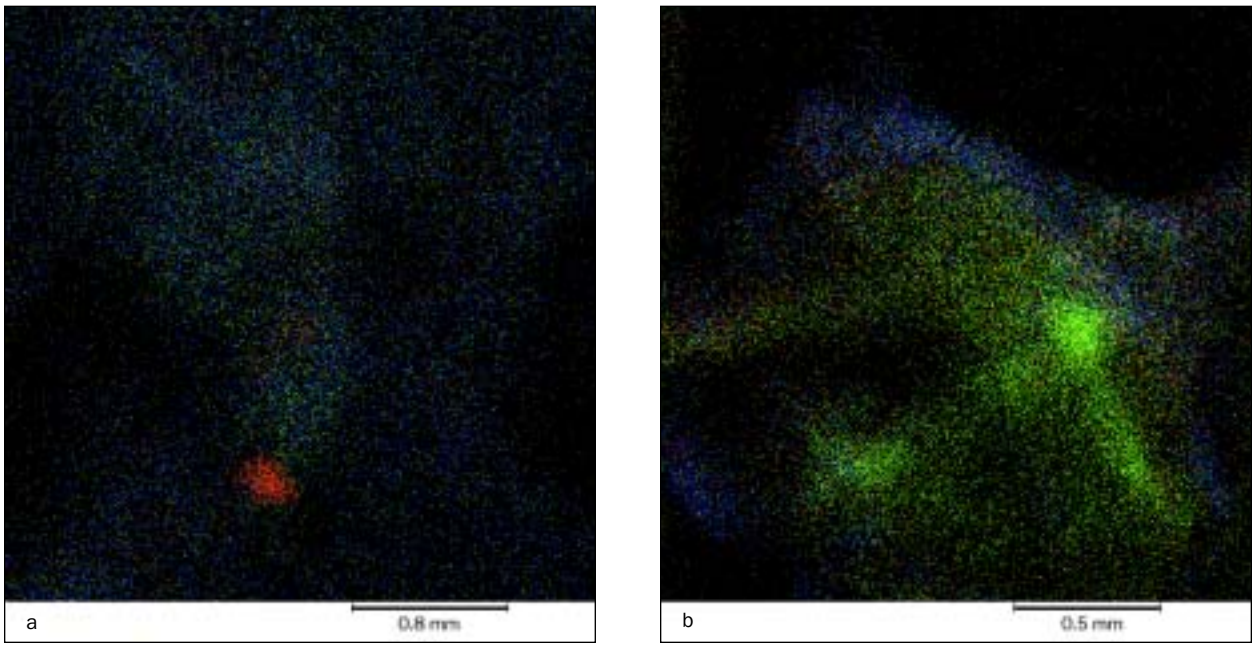

Figs 10a and 10b Images with elements superimposed (original magnification ×100) detected with the XGT. Measurement time was 900 seconds with a width (squares are mapped in mm) of 3.072 mm^2. Scanning mode (no. of frames) was 5. Focal enrichment with Ca and P. NaOH-treated films (Fig 10a): Calcium distribution is expressed as red dots. Green dots symbolize iron and blue phosphorus, expressed against a black background. Untreated films (Fig 10b): Calcium distribution image expressed as red dots. Green symbolizes zinc and blue iron expressed against a black background.

GPC showed that the average molecular weight of the PCL foils of both groups decreased from 159,000 ± 5,000 to 95,000 ± 5,000 after 2 weeks of culturing and 17 weeks of implantation. The polydispersity index ranged from 1.5 on untreated and 1.2 on NaOH-treated specimens.

DISCUSSION

The concept of GBR has become widely accepted as a successful treatment modality.[16,17] The objective of GBR is to promote bone formation in osseous defects.[3,4] The gradual shift from nonresorbable membranes to biodegradable and bioresorbable membranes represents one of the most significant trends in modern GBR treatment regimes.[9] However, the membrane is not able to induce active bone regeneration because of the lack of cellular components. The presented study suggests that a tissue-engineered periosteal cell-membrane construct is capable of inducing the formation of calcified tissue in a non-osseous environment.

The authors' interdisciplinary group[18] has developed a PCL film as thin as 5 μm, which has potential to be used as a matrix for tissue-engineering applications. PCL is an FDA-approved, bioresorbable, biocompatible polymer, and has good mechanical properties when biaxially stretched. Biaxially stretched PCL films support the attachment and proliferation of human dermal fibroblasts as well as keratinocytes

and have potential to be used as matrix material when tissue engineering skin.[18]

The study presented in this paper showed that ultrathin PCL films also support cell attachment and proliferation of human calvarial osteoblasts. The NaOH treatment of biaxially stretched PCL films resulted in a microtextured, hydrophilic polymer surface that enhanced cell attachment and migration. The tissue-engineered PCL film/cell constructs were able to produce and deposit mineralized matrix. The concept of tissue engineering by combining the cellular component with a bioresorbable membrane offers a variety of new strategies for GBR. The osteoblast-biomaterial interphase has been the focus of many studies.[19,20] In particular, interest has been focused on cell attachment and subsequent formation of mineralized tissue.[21]

Cell attachment and migration are dependent on cell/substrate interaction. The surface properties of the material have a strong biophysical influence on the cell kinetics. Osteoblasts are an anchorage-dependent cell type and need to attach and spread so as to divide and become confluent. The cytoskeletal response (actin filament and focal contact formation) of osteoblast-like cells to various substrates has been studied by many investigators and was reviewed by Anselme.[22] Nonbiomolecular scaffold surface engineering refers to the altering of a material's cell attachment and proliferation performance by modifying the polymer end groups to afford a higher affinity for protein adsorption.

A procedure for surface hydrolysis of polyglycolic acid (PGA) meshes was developed by Gao and coworkers[23] to increase cell seeding density and improve cell attachment. Hydrolysis of PGA in 5 mol/L NaOH transformed ester groups on the surface of PGA fibers to carboxylic acid and hydroxyl groups. However, the molecular weight and thermal properties of the polymer did not change significantly following surface hydrolysis. In cell-seeding experiments, a surface-hydrolyzed mesh could be seeded with more than twice as many cells as the unmodified PGA mesh. Control experiments indicated that adsorption of serum proteins onto the surface-hydrolyzed PGA fibers correlated with an increase in the cell seeding density.[23]

In an attempt to build on the work of Gao and colleagues,[23] the surfaces of the PCL membranes were modified using NaOH treatment. Specific matrix surfaces might be capable of influencing the differentiation of osteoblast-like cells. Previous studies showed that changes in surface morphology can act as a nucleation point for matrix formation and mineralized nodule production when culturing osteoblasts.[24–26] Modified surface characteristics might lead to a different numeric and preferential absorption of proteins but also influence the conformational state of the absorbed proteins. Hasegawa and coworkers[25] demonstrated that the conformational state of proteins can influence cell activity and consequently ECM formation. This might be one of the reasons why cells, because of more favorable spreading reaction, increased their rate of growth and supported the formation of mineralized matrix in the treated samples. Mechanically transduced signals might trigger calcified globuli formation.

Osteogenesis on bioactive substrates is characterized by a temporal sequence of biologic events involving cell morphology, proliferation, and differentiation. Recent studies[27,28] have shown that apoptosis is a significant feature of osteoblast differentiation during the development of bone-like tissue. An increase of apoptosis during the growth phase in vitro could therefore suggest that the substrate induces remodeling within the osteoblast population to support the selection process of a subpopulation that can adapt to the substrate-specific microenvironment. This could explain why the onset of apoptosis on the foils after 5 to 7 days in culture was detected, although confluence was not yet reached and cell proliferation continued (Figs 3c and 3d).

The combined immunohistochemical staining indicated that the NaOH-treated PCL films in particular were able to support bone-like tissue growth. The cells that proliferated were of the intended phenotype and were able to deposit a partially mineralized ECM in vivo. The von Kossa assay test for calcium, in the presence of phosphate, is a general measure of mineralization of the ECM.

The nondestructive imaging of elemental distribution of tissue-engineered hard tissues provides valuable information to complement histologic and immunohistochemical methods. The ratio of elements that form the mineralized extracellular matrix in hard tissue is important. To the authors' knowledge, this is the first published report applying that method to tissue engineered specimens. The information obtained from the tissue analysis with the XSAM supported the findings from the overall histology. Even so, the scanned planes could not be precisely adjusted to the histologic sections. However, variations in distribution of mineralized areas can be explained by the technical limitations of the currently available XSAM. The new generation of XSAMs will allow a more specific application when analyzing biologic specimens.[15]

Bioresorbable and biodegradable membranes for GBR were introduced towards the end of the 1980s.[9] Products consisting primarily of PGA and polydiaxannone were used. These materials have in common a short degradation time. After a primary

hydrolytic breakdown into lactic acid and glycolic acid, these materials are further broken down into carbon dioxide and water in the citrate cycle. This is often accompanied by a mild inflammatory reaction, creating an acidic environment, which is not ideal for early tissue development. Pitt and colleagues[29] were among the first who observed that in vivo biodegradation of nonporous PCL specimens proceeded in 2 stages. The first stage of the degradation process involves non-enzymatic, random hydrolytic ester cleavage, and its duration is determined by the initial molecular weight of the polymer as well as its chemical structure. The second phase is characterized by the onset of mass loss. Mass loss has been attributed to that chain scission of low-molecular-weight compounds which will produce oligomers small enough to diffuse out of the polymer's bulk and surface, which can then be completely metabolized via phagocytosis.

GPC was employed to study the degradation kinetics of the PCL film/cell constructs. The molecular weight of the seeded PCL matrices decreased significantly over 17 weeks. Perhaps the best representation of the change in molecular weight was visible in the polydispersity index (PI). High PI values correspond to a conglomerate of chains spanning a wide range of molecular weights. The membranes initially had a low PI value, which indicates a homogeneous distribution of molecular chains of the same size. During cell implantation, the longer molecular chains were cut via hydrolysis, but the PI did not change significantly, indicating a gradual degradation process. Based on these data it can be extrapolated that the degradation characteristics of biaxially stretched PCL films fulfill the criteria for GBR where the polymer matrix should stay intact for 4 to 6 months.[9] Conclusively, the results of this study indicate that biaxially stretched PCL films support the attachment and proliferation of osteoblast-like cells and have potential for use in developing a new generation of truly osteoinductive membranes.

ACKNOWLEDGMENTS

The authors thank Professor Mary Ng and Patricia Netto from the Electron Microscopy Unit at the National University of Singapore for characterizing the specimen with the XSAM. Also, M. Lian Hock Chuan from Horiba Instruments Singapore is thanked for providing the XSAM.

REFERENCES

1. Mellonig JT, Nevins M. Guided bone regeneration of bone defects associated with implants: An evidence-based outcome assessment. Int J Periodontics Restorative Dent 1995;15:169–184.
2. Hutmacher D, Kirsch A, Ackermann KL, Liedtke H, Huerzeler MB. GBR treatment concepts: Membrane fixation and stabilization with bioresorbable minipins. Implantologie 1998;3:117–135.
3. Buser D, Dula K, Hirt HP, Schenk R. Lateral ridge augmentation using autografts and barrier membranes: A clinical study with 40 partially edentulous patients. J Oral Maxillofac Surg 1996;54:420–432.
4. Linde A, Alberius P, Dahlin C, Bjurstam K, Sundin Y. Osteopromotion. A soft tissue exclusion principle using a membrane for bone healing and bone neogenesis. J Periodontol 1993;64:1116–1128.
5. Dahlin C, Andersson L, Linde A. Bone augmentation at fenestrated implants by an osteopromotive membrane technique. A controlled clinical study. Clin Oral Implants Res 1991;2:159–165.
6. Schenk RK, Buser D, Hardwick WR, Dahlin C. Healing pattern of bone regeneration in membrane-protected defects. Int J Oral Maxillofac Implants 1994;9:13–29.
7. Gottlew J. Guided tissue regeneration using bioresorbable and non-resorbable devices: Initial healing and long-term results. J Peridontol 1993;64:1157–1165.
8. Hardwick R, Hayes KB, Flynn C. Devices for dentoalveolar regeneration: An up-to-date literature review. J Peridontol 1995;66:495–505.
9. Hutmacher D, Huerzeler MB, Schliephake H. A review of material properties of biodegradable and bioresorbable polymers and devices for GTR and GBR applications. Int J Oral Maxillofac Implants 1996;11:667–678.
10. Hutmacher DW, Kirsch A, Ackermann KL, Huerzeler MB. A tissue engineered cell occlusive device for hard tissue regeneration—A preliminary report. Int J Periodontics Restorative Dent 2001;21:48–59.
11. Langer R, Vacanti JP. Tissue engineering. Science 1993; 260:920–926.
12. Mikos AG, Bao Y, Cima LG, Ingber DE, Vacanti JP, Langer R. Preparation of polyglycolic acid bonded fiber structures for cell attachment and transplantation. J Biomed Mater Res 1993;27:183–189.
13. Ng CS, Teoh SH, Chung TS, Hutmacher DW. Simultaneous biaxial drawing of polycaprolactone films. Polymer 2000;41:5855–5864.
14. Breitbart AS, Grande R, Kessler JT, Ryaby RJ, Fitzsimmons RT, Grant T. Tissue engineered bone repair of calvarial defects using cultured periosteal cells. Plast Reconstr Surg 1998;101:567–576.
15. Uo M, Watari F, Yokoyama A, Matsuno H, Kawasaki T. Dissolution of nickel and tissue response observed by X-ray scanning analytical microscope. Biomaterials 1999;20: 747–755.
16. Heard RH, Mellonig JT. Regenerative materials: An overview. Alpha Omegan 2000;4:51–58.
17. Buser D, Meier E, Magnin P, Rees TD. Therapy possibilities and current treatment concepts. Schweiz Monatsschr Zahnmed 2001;111:170–187.

18. Ng KW, Hutmacher DW, Schantz JT, et al. The evaluation of ultra-thin Polycaprolactone films for tissue engineering skin. J Tissue Eng 1997;4:441–455.
19. Ishaug SL, Payne RG, Yasemski MJ, Aufdemorte TB, Bizios R, Mikos AG. Osteoblast migration on Polyhydroxyesters. Biotech Bioeng 1996;50:443–451.
20. Matsuka K, Walboomers XF, De Ruijter JE, Jansen JA. The effect of poly-L-lactic acid with parallel surface micro groove on osteoblast-like cells in vitro. Biomaterials 1999; 20:1293–1301.
21. Dalton BA, Mc Farland CD, Underwood PA, Steele JG. Role of heparin binding domain of fibronectin in attachment and spreading of human bone-derived cells. J Cell Sci 1995;108:2083–2092.
22. Anselme K. Osteoblast adhesion on biomaterials. Biomaterials 2000;21:667–681.
23. Gao J, Niklason L, Langer R. Surface hydrolysis of polyglycolic acid meshes increases the seeding density of vascular smooth muscle cells. J Biomed Mater Res 1998;42:417–424.
24. Xynos ID, Hukkanen MVJ, Batten JJ, Buttery LD, Hench LL, Polak JM. Bioglass 45S5 stimulates osteoblast turnover and enhances bone formation in vitro: Implication and application for bone tissue engineering. Calcif Tissue Int 2000; 67:321–329.
25. Hasegawa T, Oguchi H, Mizuno M, Kuboki Y. The effect of the extracellular matrix on differentiation of bone marrow stromal cells to osteoblasts. Jpn J Oral Biol 1994:383–394.
26. Kieswetter K, Schwartz Z, Dean DD, Boyan BD. The role of implant surface characteristics in the healing of bone. Crit Rev Oral Biol Med 1996:7:329–345.
27. Lynch MP, Capparelli C, Stein JL, Lian JB. Apoptosis during bone-like tissue development in vitro. J Cell Biochem 1998;68:31–49.
28. Fratzl-Zelman N, Horandner H, Luegmayr E, et al. Effects of triiodo-thyronine on the morphology of cells and matrix, the localization of alkaline-phosphatase and the frequency of apoptosis in long-term cultures of MC3T3-E1 cells. Bone 1997; 20:225–231.
29. Pitt CG, Chasalow FI, Hibionada YM, Klimas DM, Schindler A. Aliphatic polyesters I: The degradation of polycaprolactone in vivo. J Appl Poly Sci 1981;26:3779–3787.